Cyclodextrins as a Templating Agent in Solvent-Free Kneading- Based Syntheses of Nanosized SnO2 and ZnO

This is a pre print version of the following article:

Original Citation:

Availability:

This version is available http://hdl.handle.net/2318/1874582   since   2022-10-04T13:23:30Z

Published version:

DOI:10.1021/acssuschemeng.2c02344

Terms of use:

Open Access

(Article begins on next page)

07 January 2023

Cyclodextrins as templating agent in solvent-free kneading-based syntheses of Nanosized SnO$_2$ and ZnO

1
2
3
4 *Alberto Rubin Pedrazzo[a]*, Andrea Jouve[a], Sara Morandi[a], Maela Manzoli[b], Claudio Cecone[a],*

5 *Pierangiola Bracco[a] and Marco Zanetti[a,c]*

6

7 [a]Department of Chemistry, University of Torino, Via P. Giuria 7, NIS and INSTM Reference

8 Centres University of Torino, 10125 Torino, Italy

9 [b]Department of Drug Science and Technology, NIS and INSTM Reference Centres University of

10 Torino, Via Giuria 9, 10125 Torino, Italy

11 [c]ICxT Centre, University of Torino, Lungo Dora Siena 100, 10153 Torino, Italy

12

13 KEYWORDS

14 Kneading, cyclodextrins, MOS, semiconductor metal oxides, mechanochemistry

15 ABSTRACT

16 ------

INTRODUCTION

In recent years, gas sensors have been increasingly used in industrial production and daily life:

efficient, low cost and small-sized sensors are nowadays requested in many fields of applications

such as environmental, food or biomedical [REF].

In this context, in the ultra-sensible sensors field there has been a growing interest and diffusion

of metal oxide-based semiconductors (MOS): MOS are suitable materials for sensors for their

outstanding physical and chemical properties that combine high efficiency, fast response, stability

and, last but not least, simple preparation and low cost. [1,2]

In gas sensing applications (and in solar cell and photo-catalysis as well) MOS activity is strongly

related to the specific surface area [3,4]. To improve the properties of MOS and, consequentially, to

improve efficiency of semiconductor metal oxides-based devices, research is nowadays moving

towards nano-sized structures with controllable crystalline phases.

There are many examples of synthetic methods for obtaining ceramic nanoparticles, such us

thermal and physical deposition, hydro/solvo-thermal processes[5,6] and, over the last few years,

electrospinning (ES) [7–14].

ES is a widespread and relatively simple technique to obtain both micro and nano fibers of

polymers usually showing high porosity and high specific surface area [15–17]. Recently[18,19], our

research group adopted the procedure of electrospinning of polymeric solutions containing

precursors of ceramics, followed by thermal treatment, for the obtaining of ceramic nanofibers.

The addition of an oxide precursors to the ES solutions and a subsequent thermal treatment, above

the thermal degradation of the polymer, will ablate the polymer and, at the same time, convert the

precursor in the respective oxide[10,20–22]. Our last work in this field was focused on the influence of

the polymer on morphology and microstructure[18], confirming the concept of the polymer as a

40   templating agent, but also as variable capable of influencing morphological properties and the size

41   of the final oxide particles. In this work we are proposing a new synthetic route of nanosized MOS,

42   based on the same combination of oxide precursors and polymers (in this case oligomers) as

43   templating agent, exploiting a more simple and fast approach that does not involve an

44   electrospinning step. The ES, before calcination, is indeed replaced by the simple kneading of the

45   precursors in presence of an excess of cyclodextrins.

46   Cyclodextrins (CDs) are a family of cyclic oligosaccharides, composed of α-D-glucopyranose

47   units linked through α -1,4 glycosidic bonds, with a peculiar toroidal structure[23]. CDs are obtained

48   from enzymatic conversion of starch and are renewable and eco-friendly materials. Moreover CDs

49   are biocompatible and biologically degradable[24–26]. The three major and relevant from the

50   industrial point of view representatives of CDs family are the α-CD, β-CD and γ-CD and are

51   composed of 6, 7 and 8 glucopyranose units, respectively.[24,26–28]. The CDs structure, with the

52   presence of a slightly apolar cavity and a hydrophilic external part, determines the ability to

53   establish specific interactions with various types of molecules through the formation of

54   noncovalently bonded complexes, either in the solid phase or in aqueous solution. There are many

55   examples in literature of CDs complexes with many different organic compounds [24,27,29,30] or metal

56   ions[31,32] and cyclodextrins are extensively used in a wide range of applications[26,33].

57   In 2016 [34], Zhang *et al.* employed host-guest inclusion complexes as versatile (the chemical

58   composition of host-guest inclusion complexes can be finely tuned) precursors for obtaining

59   hetero-doped carbon materials.

60   The present work demonstrates the possibility to exploit inclusion complexes of CDs and metal

61   precursors to obtain nanostructured oxide: cyclodextrins plays in this case the role of a sacrificial

62   template. We selected precursors of SnO_2 and ZnO (two MOS traditionally obtained in form of

63 nanostructures via sol-gel synthesis or, as said, more recently, via electrospinning) because they

64 have been widely investigated in solar cells, photocatalysts and gas sensors [6,19,35,36]: the inclusion

65 complexes were prepared using Zinc Oxide (ZnAc) and Tin (II) - ethylexanoate (SnEx) and

66 exploiting a sustainable and solvent-free approach, completely based on the simple kneading of α-

67 CD, β-CD and γ-CD and precursors in ball mill.

68 According to the Green Chemistry Principles, published in 1998 by Anatastas *et al.*, chemical

69 processes must be designed in order to "minimize the quantity of final waste and to avoid

70 hazardous or toxic solvents". [37,38] Unfortunately, toxic solvents are present in most of processes:

71 the recovery and reuse are often expensive, and the disposal is a major concern. Even if in much

72 smaller quantities, the process reported in our previous article[18] for obtaining oxides with

73 electrospinning also involves the use of dimethylformamide for the preparation of the polymeric

74 solution to be electrospun.

75 The use of kneading for the preparation of inclusion complexes with CDs is quite established,

76 permitting to overcome all the limitations related to poorly soluble or insoluble compounds[29,39,40];

77 in our case permitted to completely avoid the use of solvents and to speed-up the preparation of

78 the MOS precursor.

79 The complexes after kneading were characterized by thermogravimetric analyses and,

80 subsequentially, thermally treated for the obtaining of the oxide. After the synthesis the so obtained

81 SnO_2 and ZnO nanoparticles were characterized by scanning electronic microscopy (SEM), high-

82 resolution transmission electron microscopy (HR-TEM) and by X-ray diffraction (XRD) and by

83 measuring the BET surface area, evidencing a possible influence of the CDs dimension on the

84 finale oxide.

85

EXPERIMENTAL

87 *Materials*

88 β-CD were provided by Roquette Frères (Lestrem, France) with purity > 95%. α-CD, γ-CD

89 (research grade, purity > 95.0%) were purchased from Cyclolab (Budapest, Hungary) .

90 Cyclodextrins were dried in oven at 75 °C up to constant weight, before use.

91 SnO_2 and ZnO precursors, respectively Tin(II) 2-ethylhexanoate (SnEx, purity grade of 94.4%)

92 and Zinc Acetate (dihydrate, ZnAc), were purchased from Sigma-Aldrich (Steinheim, Germany)

93 and used without further purifications.

94

95 *Ball Mill (BM)*

96 The ball mill used for the kneading step was a Retsch PM200 High Speed Planetary Ball Mill

97 (Haan, Germany), with planetary configuration and Zirconia jars, inner volume 50 mL.

98

99 *Thermogravimetric analyses*

100 Thermogravimetric Analyses (TGA) were performed on a TA Instruments (New Castle, DE, USA)

101 Hi-res Q500 Thermogravimetric Analyzer. TG Analyses parameters are the same for all samples:

102 100 mL/min air-flow, heating rate 10 °C/min, RT to 700 °C. The thermograms were elaborated

103 using TA Instruments Universal Analysis 2000 software and, subsequentially, OriginLab2019b.

104

105

106

107

108 *Preparation of the samples*

109   The preparation is the same for all oxides samples and can be divided in 2 parts:

110

111   *Kneading:* an appropriate amount of cyclodextrins (dried powder) is kneaded with the precursor,

112   approximately respecting the molar ratio 2:1, expressing an excess of cyclodextrins.

113   For Tin(II) 2-ethylhexanoate (viscous liquid): 3 g of α-CD, kneaded with 0.624 g of SnEx; 3 g of

114   β-CD, kneaded with 0.535 g of SnEx; 4 g of γ-CD, kneaded with 0.624 g of SnEx.

115   For Zinc Acetate (powder): 3 g of α-CD, kneaded with 0.338 g of ZnAc; 3 g of β-CD, kneaded

116   with 0.290 g of ZnAc; 4 g of γ-CD, kneaded with 0.338 g of ZnAc.

117

118   The mixtures are kneaded for 1 h at 300 rpm. The size of the balls is 5 mm (declared diameter).

119   Approximately 12 mL (volume, measured with graduated cylinder) of sintered zirconium oxide

120   balls, 5 mm of diameter, in each jar. Quantities of kneaded reactants are optimized for this specific

121   volume of balls and, consequently free volume in the jars.

122

123   *Calcination/Elimination of Organic Fraction*: after calcination all samples were thermally treated

124   to eliminate the cyclodextrin matrix and convert the precursor into the correspondent oxide.

125   In a typical procedure approximately 8-10 g of mixture cyclodextrin/precursor contained in a

126   Coors combustion boat were inserted in a Lenton (Hope, UK) tubular furnace.

127   Parameters were optimized via Thermogravimetric Analyses; used conditions were the following:
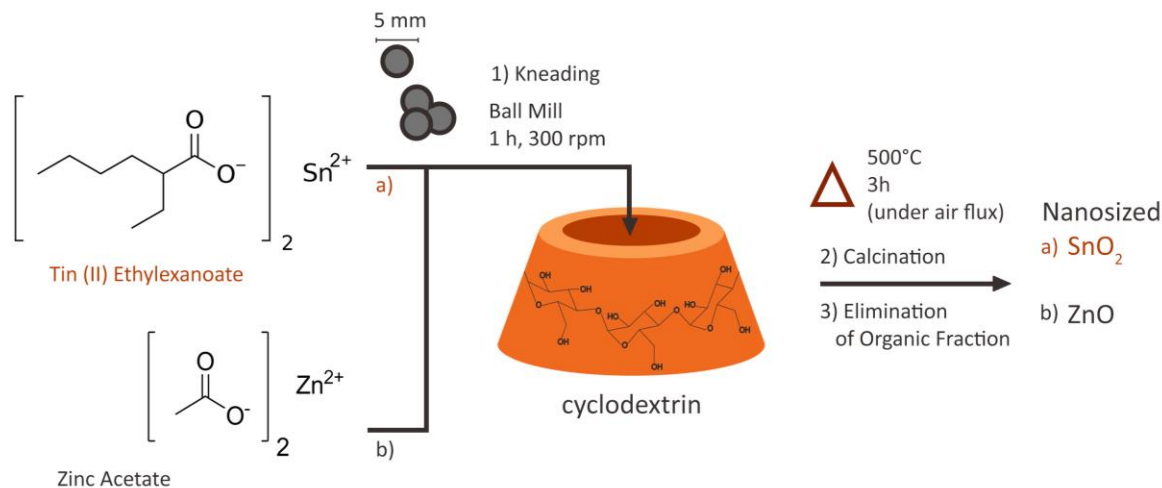
128   3h, 500° C, under 100 mL/min air-flow.

129   A white powder was obtained from all thermal treatments.

130

131   Scheme 1, following, shows a schematic representation of the complete procedure.

132   Further details of the synthesis will be discussed more in deep in the next sections (Results and

133   Discussion).

134

Scheme 1 - Schematic representation of the proposed kneading-based approach

136

137   .

138

139   *X-ray diffraction*

140   X-ray diffraction (XRD) patterns of samples SnO_2 and ZnO obtained after thermal treatment were

141   collected to determine the crystalline phases and the average crystallite sizes by applying the

142   Scherrer's formula on the (xxx) diffraction peak.

143   XRD) analysis were carried out on a PW3050/60 X'Pert PRO MPD (PANalytical, Malvern, United

144   Kingdom), using as X-ray source a PW3373/10 LFF with Cu Anode, $\lambda = 0.541$ Å.

145

146   *BET*

147   Gas-volumetric analysis Nitrogen adsorption–desorption isotherms were measured using a

148   Micromeritics ASAP2010 volumetric sorption analyzer (Norcross, GA, USA). Before

149 measurements, the samples were outgassed at 100 °C under vacuum (10 mm Hg) for 15 hours (for

150 removing water and eventual adsorbates). The specific surface areas were determined through the

151 Brunauer-Emmett-Teller (BET) method to the adsorption/desorption isotherms of N_2 at 77 K.

152

153 *SEM*

154 Morphological characterization of the samples was performed by scanning electron microscopy

155 (SEM), using a Tescan VEGA 3 SEM (Brno, Czech Republic) working with secondary electrons

156 and 10keV accelerating voltage. The samples were analyzed without any previous metal coating.

157

158 *TEM*

159 High-resolution transmission electron microscopy (HR-TEM) was utilized to achieve further

160 morphological and structural information: the instrument is a Jeol (Akishima, Tokyo, Japan) JEM

161 3010 UHR (300 kV, LaB6 filament). The synthesized samples were deposited on a Cu grid, coated

162 with a porous carbon film. All digital micrographs were acquired by an Ul-traSscan 1000 camera,

163 and the images were processed by Gatan digital micro-graph (Pleasanton, CA, US) .

164

165

166

167

168

169 RESULTS AND DISCUSSION

170 The starting point for this project is the idea of using a polymer as a sacrificial template to obtain

171 very small oxide particles for specific applications. The focus is therefore on the final resulting

172 oxide but, as we recently demonstrated [18], the influence of the polymer on the precursor conversion

173 is dramatic. The choice of the templating polymer, consequentially, is of primary importance. Our

174 choice fell on cyclodextrins for different reasons: CDs are a widely studied oligomer [25], with an

175 extensive literature that supports many of our claims, CDs are a renewable because obtained from

176 enzymatic conversion of starch [24,25]. Thus, CDs are renewable, eco-friendly materials and, last but

177 not least, cheap. In Figure 1, following, are reported a simplified chemical structure of a α, β and

178 γ CDs and the respective dimensions of the CDs employed in the present work.
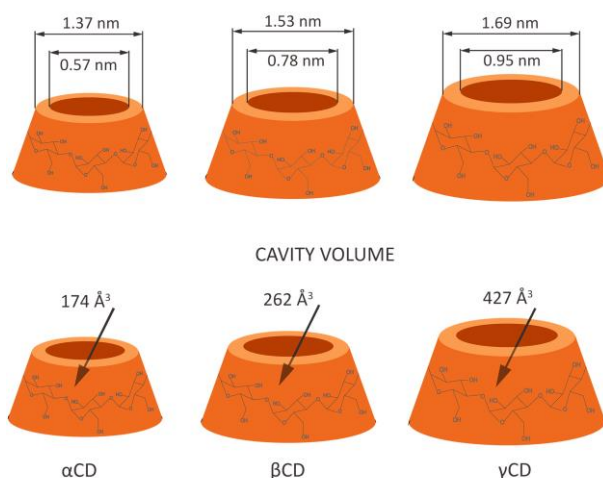
179

180 **Figure 1 - Simplified structure and dimensions of α, β and γ cyclodextrins**

181

182 α, β and γ cyclodextrins exhibit a different size and a different cavity volume (Figure 1, details).

183 The principle behind exploiting CDs as a sacrificial "container" is also associated the relatively

184 high degradation temperature of the pristine CDs, that is roughly around 300°C for α, β and γ

185 cyclodextrins: this is a crucial parameters, because the polymer "matrix", in this case the oligomer,

186 needs to be completely removed in an efficient way, but still needs to protect e to assist in a

187 synergic way the formation of the oxide. In order to obtain the SnO_2 and ZnO, it is necessary to

188 achieve the complete volatilization of the polymer and the degradation organic precursor [19]. An

189 incomplete elimination of the organic fraction will lead to a grey/black powder, with an amorphous

190 carbon residue. At the same time, a high temperature can affect the final size of the oxide, which

191 could favor crystal growth during calcination rather than nucleation, leading to bigger particle and

192 lower surface area. In Table 1, following, are reported all the synthetic information and the BET

193 surface area, $[m^2/g]$. A careful correlation of the results shown in Table 1 with the thermal

194 measurements shown in Figure 2 and Figure 3 (and with data already present in literature), allows

195 us to make some assumptions.

196

197 **Table 1 – Oxides (α, β and γ SnO₂ and α, β and γ ZnO), relative preparative conditions (kneading step and**
198 **subsequential thermal treatment) and BET Surface Area (m²/g)**

| OXIDE		Precursor	Kneading	Thermal Treatment	BET Surface Area [m^2/g]
SnO$_2$	α-SnO$_2$	Tin (II) ethylexanoate	1 h 300 rpm 5,0 mm Ø balls 10 min inversion time	3 h 500°C ramp 10 °C/min	44,2
	β-SnO$_2$				47,1
	γ-SnO$_2$				50,4
ZnO	α-ZnO	Zinc Acetate	1 h 300 rpm 5,0 mm Ø balls 10 min inversion time	3 h 500°C ramp 10 °C/min	12,0
	β-ZnO				10,5
	γ-ZnO				17,5

199

200 As shown in Table 1, the preparative conditions are the same for all samples: nevertheless,

201 outcomes are quite different. The BET Surface area for what concerns the SnO₂ is comprised

202 between ≈ 44 and 50 m²/g, for all CDs template, a quite interesting result, comparable with the

203 results reported in the literature with oxides and similar treatments REF. It is necessary to

204 underline, however, that these very interesting results were obtained through an objectively very

205 simple preparation, without complex procedures and, even more noteworthy, without any solvent

206   in any step. However, the same reasoning cannot be made with regard to ZnO. The oxide obtained

207   has a much lower surface area, indeed. SnO_2 and ZnO are certainly two completely different oxides

208   but the dramatic difference in the final result is clear. Still, the presence of a trend in both oxides

209   from different precursors is evident: the surface area appears to be (with the sole exception of β-

210   ZnO, Table 1 for reference) inversely proportional to the size of the cyclodextrin cavity. It is worth

211   to say that the formation of an inclusion complex is not the only possible way of CDs to form

212   complexes: stable interactions are sometimes established between a guest molecule and the

213   external part of CDs. Indeed, hydroxy group on the outer surface of cyclodextrins can lead to the

214   formation of hydrogen bonds and, consequentially, to water-soluble complexes, in a similar way

215   to what is seen with non-cyclic oligo or polysaccharides [27,41]. These supramolecular assemblies

216   (there are no covalent bonds) are called *non-inclusion* complexes. They can, eventually, protect

217   guest molecules from the environment and achieve anyway an efficient increase of solubility. In

218   literature many examples of non-inclusion compounds are reported [42–45]. Among the others there

219   is, of course, the size compatibility between host and guest molecules. The size of CD has to be

220   large enough to permit the guest entrance but if the guest is too small if compared to the cavity,

221   CD-guest interactions will be very weak, and the dissociated form will prevail on the associated

222   one. The same applies for the opposite situation: a molecule larger than the cavity will enter

223   partially or will arrange outside the cavity. An example in literature is, for example, the

224   naphthalimide, where the apolar chain fit preferentially in a smaller α-cyclodextrin cavity, wherein

225   the aromatic moiety of the same molecule will arrange inside a β-cyclodextrin [46].

226   It is therefore possible to hypothesize that there is not the real formation of a 1: 1 complex, but

227   rather the formation of "clusters". Given the interesting results these clusters are necessarily of

228   small size; thus, it is possible to assume that in any case the ion or the precursor are, statistically,

229   partially or completely incorporated by the cyclodextrins and this is more probable with the γCD,

230   whereas the cavity is larger. This hypothesis can also be supported by a possible interpretation of

231   the thermogravimetric analyses, Figure 2 and Figure 3, following.

232
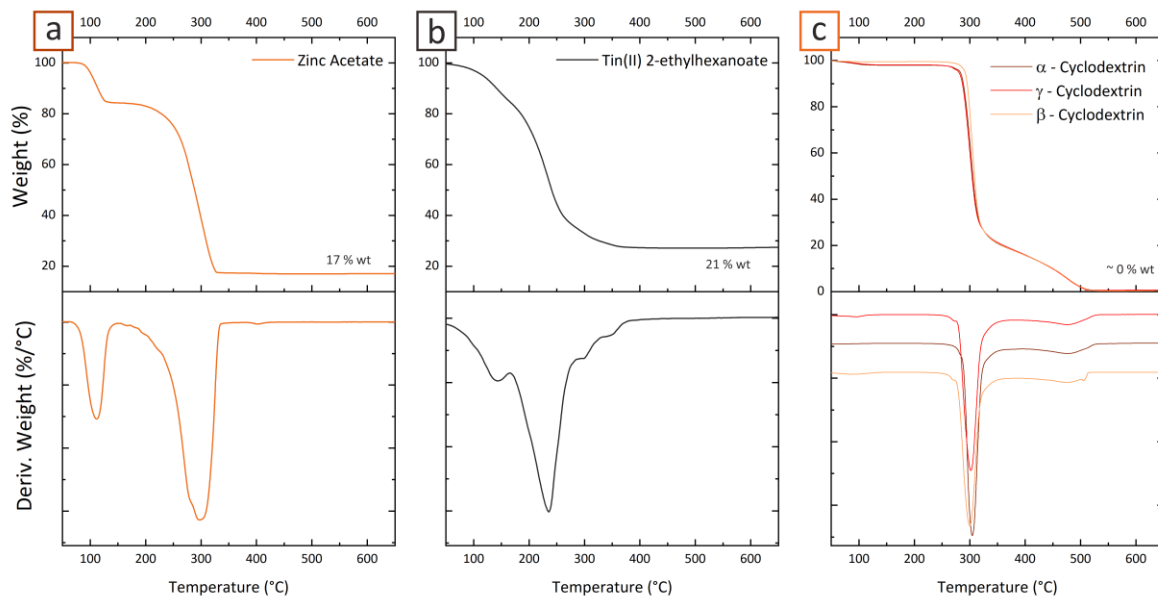
Figure 2 - Comparison of thermo-gravimetric analysis (TGA) and derivative TGA (DTGA) of the different component of the precursor mixture in air, from RT to 700 °C, 10 °C/min. Respectively a) Zinc Acetate b) Tin (II) ethylexanoate c) α, β and γ Cyclodextrins

236
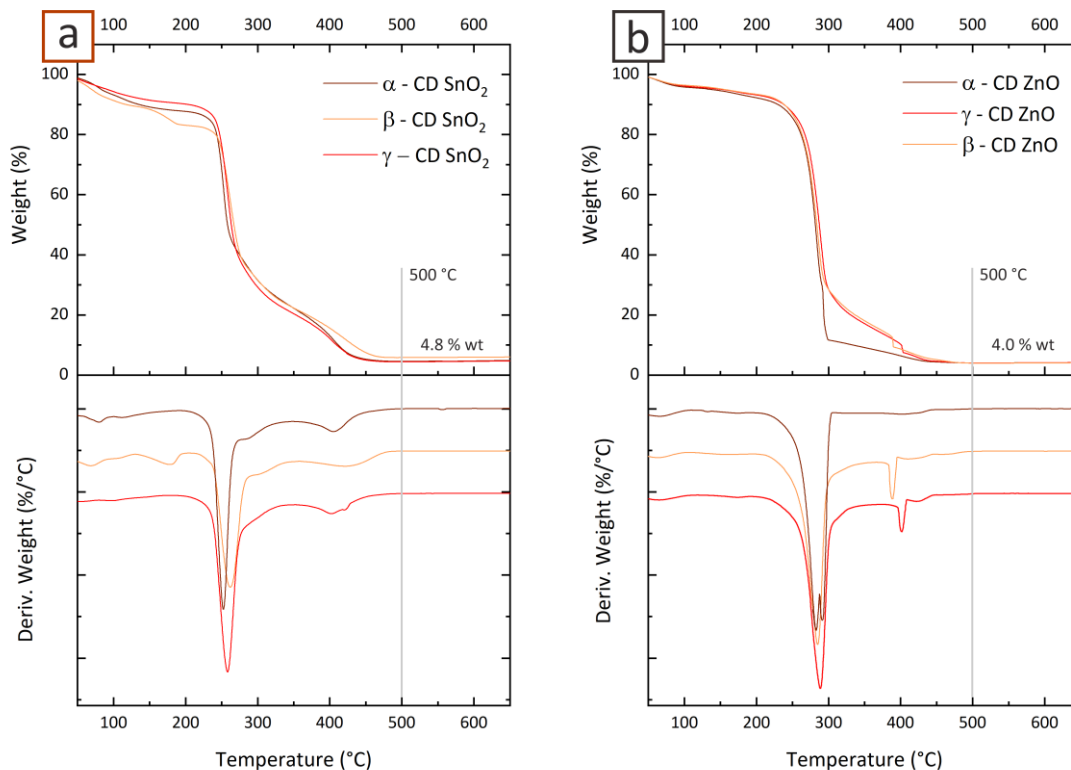
Figure 3 - Comparison of thermo-gravimetric analysis (TGA) and derivative TGA (DTGA) ir, from RT to 700 °C, 10 °C/min. a) α, β and γ SnO₂ from Tin (II) ethylexanoate/CDs and b) α, β and γ ZnO from Zinc Acetate/CDs

In Figure 2, the thermo-gravimetric analyses and derivative TGA of the different component of the precursor mixture in air, from RT to 700 °C, are reported. The degradation of ZnAc, inset a) Figure 2, shows a thermal degradation that proceeds in two different steps: the first one at 100°C reasonably related to the water and the second one, that starts before 300°C and that leads to a residue of 17%, can be related to the decomposition of ZnAc itself, that is only partially converted into ZnO (ZnAc is reported to sublimate at 234 °C[47]). Assuming a total conversion of the precursor into ZnO the residual should amount to approximately 37% wt. A similar situation is shown with the Tin (II) ethylexanoate, inset b) Figure 2, where the residue from TG is around 21%: also in this case the expected quantity of residue, with a complete conversion of the precursor in SnO₂, is 37%.

13

250   In both precursors, there is a competition between degradation and oxidation, indeed. A different

251   situation is shown in Figure 2, inset c), concerning CDs. The degradation can be divided in three

252   stages[48]: the first one, below 100°C, due to loss of absorbed water and water of crystallization (in

253   this case, since CDs were dried for at least 24h, the weight loss is barely detectable), the second,

254   that develops in a temperature range that start at roughly 250 °C, which is associated with a weight

255   loss of 70-80%, with the formation of a char residue and the third, at T > 300 °C, that leads to

256   complete oxidation (combustion) of the residue.

257   The final residue, after the third stage, is ≈ 0% for all cyclodextrins. Cyclodextrins alone, therefore,

258   in an oxidizing atmosphere, do not leave any residue.

259   Consequentially, looking at the thermogram reported in Figure 3, showing a residue around 4.8 %

260   for SnO2 and 4.0 % for ZnO, it is possible to state that the simultaneous presence of CDs and

261   precursor leads to the formation of an oxide and that the cyclodextrins are completely eliminated

262   from the mixture above 450 ° C. In both thermograms, inset a) and b) Figure 3, most of the weight

263   loss profile is related to the volatilization of the cyclodextrin matrix, and this is consistent with

264   what it was possible to hypothesize considering the initial composition of the mixture after

265   kneading. What is necessary to highlight is the amount of residual oxide, because it could confirm

266   a protective effect of the cyclodextrins: the theoretical residue in oxide, assuming a total

267   conversion of the precursor present in the post-kneading mixture is 4.5 % for ZnO and 5.6 % for

268   SnO_2, respectively. Thus, results are remarkably close to the 4.0 % and 4.8 % reported before. The

269   yield is low, but we must consider that the precursor/CDs kneaded mixture contains approximately

270   15% wt. of precursor: tin (II) 2-ethylhexanoate and zinc acetate, if heated in the same conditions,

271   volatilize, leaving a considerably smaller amount of residue, while in this case the precursor is

272   almost completely converted into oxide.

273　Cyclodextrins, therefore, do not only play a role of simple support but rather protect and assist the

274　formation of oxide (preventing the volatilization of the precursor), influencing both its yield and

275　final size.

276　However, it is necessary to make further considerations, about the possible reasons why the same

277　interesting results, concerning the BET surface area (and consequentially particle size) were not

278　obtained as for SnO_2 with ZnO. In Figure 2 it is evident that cyclodextrins have their principal

279　weight loss at a temperature comparable to that of zinc acetate, while it is about 50 °C higher than

280　that of tin (II) 2-ethylhexanoate: given the results previously commented and assuming therefore

281　that there is a protective effect, this is effective only if the "shield" molecule does not degrade

282　before the host molecule.

283　Moreover, a less effective protective effect can also be hypothesized from an analysis of the TG

284　curves reported in inset b) of Figure 3: in the area around 400 degrees, where in presence of oxygen

285　presumably occurs the oxidation/combustion of the cyclodextrins, it is possible to notice an

286　anomalous behavior (very evident in the peaks of the first derivative). These small weight losses

287　can be related to volatiles that are quickly released as soon as the protective "cage" is thermally

288　oxidized. Given the tendency of ZnAc to sublimate, reported in the literature, it can be

289　hypothesized that part of the precursor is actually not converted but rather simply "blocked" and

290　subsequently lost during the heating.

291　Another plausible reason in the different superficial area from a comparison of the two different

292　precursors can be related to the fact that in the case of the SnO_2, the kneading phase is carried out

293　with a liquid precursor, tin (II) 2-ethylhexanoate, instead of a powder such as in the case of the

294　Zinc Acetate: the liquid form of the precursor leads to a much more effective grinding / mixing,

295 leading to the obtainment of a sort of "paste". From a practical point of view, the kneading phase

296 therefore seems to have a significant influence on the final result.

297

298 We also characterized the final oxides from the morphological point of view by scanning electron

299 microscopy, results are shown below (Figure 4):
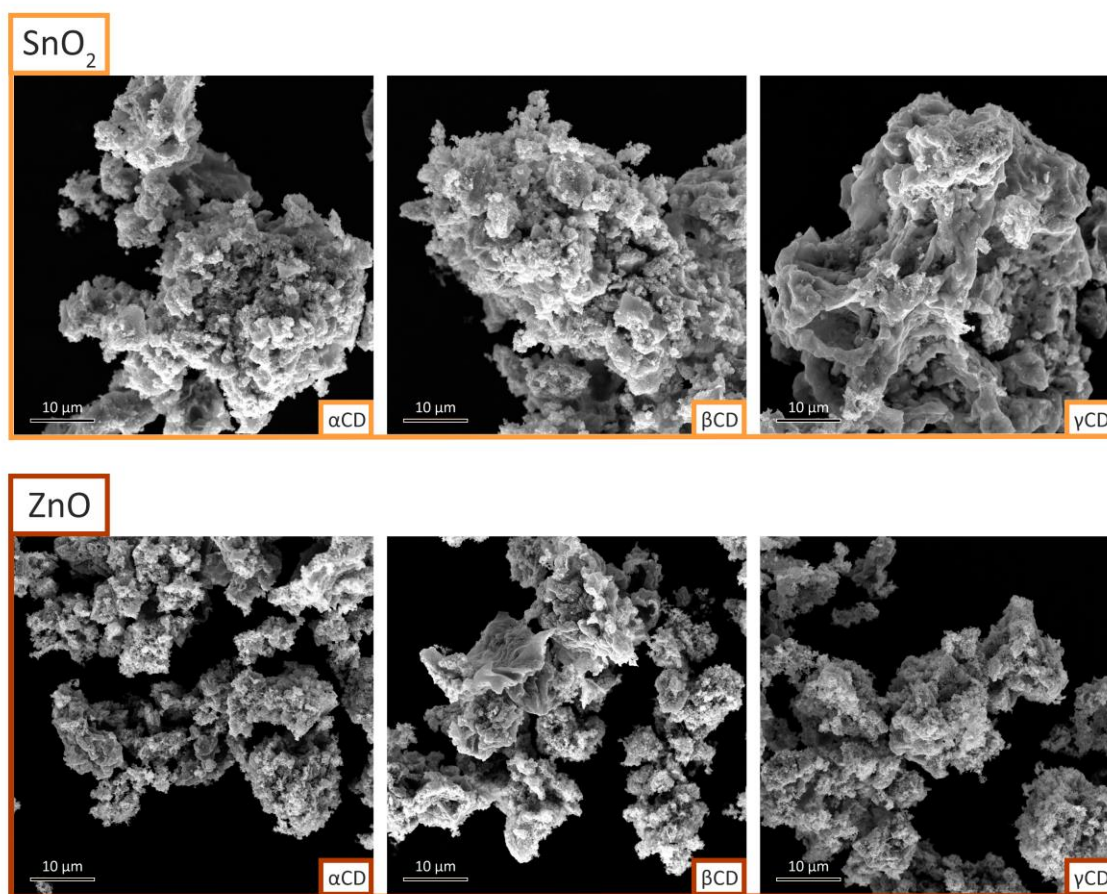
300

301 **Figure 4 SEM images of the oxide obtained from different precursors and CDs. Instrumental magnification**
302 **5kx, 10keV**

303

304 The suitable temperatures for calcining the mixture after the kneading step were chosen on the

305 results obtained by TG analyses, considering the temperatures at which the weight losses are

306 concluded: the same temperature, 500 °C was, used for the calcination of all kneaded mixtures,

16

307 leading to a white and uniform oxide residue. As shown in Figure 4, there are no particular

308 differences that emerge from the SEM comparison of the samples, even if obtained from different

309 mixtures of oxides and oligomers. Higher magnification are reported in Supporting Informations.

310
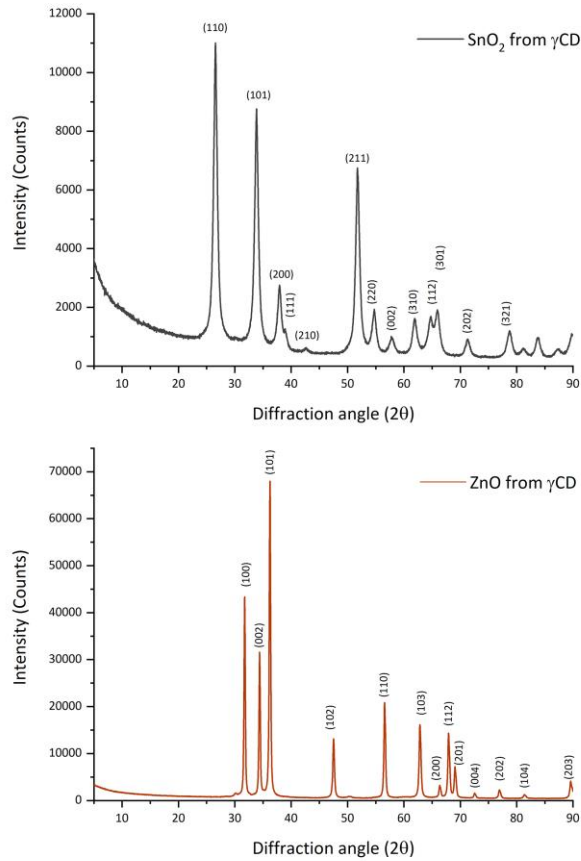
Figure 5 XRD patterns of SnO₂ and ZnO, from precursot/γCD mixtures.

The XRD confirms that the samples are constituted by crystalline cassiterite (SnO_2 in the tetragonal crystal phase, JCPDS file number 00-001-0625). The calculated size (D, via Debye-Sherrer equation) is .....

TEM

CONCLUSIONS

319

320

CORRESPONDING AUTHOR

*alberto.rubinpedrazzo@unito.it, Post-Doc Fellow

ABBREVIATIONS

αCD, alpha-cyclodextrin; βCD, beta-cyclodextrin;   γCD, gamma-cyclodextrin; BM, ball-mill;

SnEx, Tin(II) 2-ethylhexanoate; ZnAc, Zinc Acetate;

326

327

328

REFERENCES

(1)   Bracco, P., Scalarone, D., Trotta, F. Electrospun Membranes for Sensors Applications, in: Smart Membranes and Sensors: Synthesis, Characterization, and Applications. *Ed. Scrivener Publ.* **2014**, 301–336.

(2)   Eranna, G.; Joshi, B. C.; Runthala, D. P.; Gupta, R. P. Oxide Materials for Development of Integrated Gas Sensors - A Comprehensive Review. *Crit. Rev. Solid State Mater. Sci.* **2004**, *29* (3–4), 111–188. https://doi.org/10.1080/10408430490888977.

(3)   Sun, Y.-F.; Liu, S.-B.; Meng, F.-L.; Liu, J.-Y.; Jin, Z.; Kong, L.-T.; Liu, J.-H. Metal Oxide Nanostructures and Their Gas Sensing Properties: A Review. *Sensors* **2012**, *12* (12), 2610–2631. https://doi.org/10.3390/s120302610.

(4)   Zaera, F. Nanostructured Materials for Applications in Heterogeneous Catalysis. *Chem. Soc. Rev.* **2013**, *42* (7), 2746–2762. https://doi.org/10.1039/C2CS35261C.

(5)   Yu, X.; Marks, T. J.; Facchetti, A. Metal Oxides for Optoelectronic Applications. *Nat. Publ. Gr.* **2016**, *15* (4), 383–396. https://doi.org/10.1038/nmat4599.

343   (6)   Das, S.; Jayaraman, V. SnO2: A Comprehensive Review on Structures and Gas Sensors.
344   *Prog. Mater. Sci.* **2014**, *66*, 112–255. https://doi.org/10.1016/j.pmatsci.2014.06.003.

345   (7)   Li, D.; Xia, Y. Fabrication of Titania Nanofibers by Electrospinning. *Nano Lett.* **2003**, *3*
346   (4), 555–560. https://doi.org/10.1021/nl034039o.

347   (8)   Choi, S. S.; Lee, S. G.; Im, S. .; Kim, S. H.; Joo, Y. L. Silica Nanofibers from
348   Electrospinning/Sol-Gel Process. *J. Mater Sci. Lett.* **2003**, *22* (12), 891–893.

349   (9)   Morandi, S.; Cecone, C.; Marchisio, G.; Bracco, P.; Zanetti, M.; Manzoli, M. Shedding
350   Light on Precursor and Thermal Treatment Effects on the Nanostructure of Electrospun
351   TiO2 Fibers. *Nano-Structures and Nano-Objects* **2016**, *7*, 49–55.
352   https://doi.org/10.1016/j.nanoso.2016.05.003.

353   (10)   Chandraiah, M.; Sahoo, B.; Panda, P. K. Preparation and Characterization of SnO2
354   Nanofibers by Electrospinning. *Trans. Indian Ceram. Soc.* **2014**, *73* (4), 266–269.
355   https://doi.org/Doi 10.1080/0371750x.2014.923786.

356   (11)   Madhugiri, S.; Sun, B.; Smirniotis, P. G.; Ferraris, J. P.; Balkus, K. J. Electrospun
357   Mesoporous Titanium Dioxide Fibers. *Microporous Mesoporous Mater.* **2004**, *69* (1–2),
358   77–83. https://doi.org/10.1016/j.micromeso.2003.12.023.

359   (12)   Bazargan, A. M.; Fateminia, S. M. A.; Ganji, M. E.; Bahrevar, M. A. Electrospinning
360   Preparation and Characterization of Cadmium Oxide Nanofibers. *Chem. Eng. J.* **2009**, *155*
361   (1–2), 523–527. https://doi.org/10.1016/j.cej.2009.08.004.

362   (13)   Dai, Y.; Liu, W.; Formo, E.; Sun, Y.; Xia, Y. Ceramic Nanofibers Fabricated by
363   Electrospinning and Their Applications in Catalysis, Environmental Science, and Energy
364   Technology. *Polym. Adv. Technol.* **2011**, *22* (3), 326–338. https://doi.org/10.1002/pat.1839.

365   (14)   Masa, S.; Hontanon, E.; Santos, J. P.; Sayago, I.; Lozano, J. Chemiresistive Sensors Based
366   on Electrospun Tin Oxide Nanofibers for Detecting NO2 at the Sub-0.1 Ppm Level. *Proc.*
367   *2019 5th Exp. Int. Conf. exp.at 2019, 2019, Funchal, Madeira Island, Port.* **2019**, No. 2,
368   310–314. https://doi.org/10.1109/EXPAT.2019.8876485.

369   (15)   MacDiarmid, A. G.; Jones, W. .; Norris, J. D.; Gao, J.; Johnson, A. T.; Pinto, N. J.; Hone,
370   J.; Han, F. K. Electrostatically-Generated Nano Fibers of Electronic Polymers. *Synth. Met.*
371   **2001**, *119* (1–3), 27–30.

372   (16)   Theron, S. A.; Zussman, E.; Yarin, A. L. Experimental Investigation of the Governing
373   Parameters in the Electrospinning of Polymer Solutions. **2004**, *45* (2004), 2017–2030.
374   https://doi.org/10.1016/j.polymer.2004.01.024.

375   (17)   Liu, S.; White, K. L.; Reneker, D. H. Electrospinning Polymer Nanofibers with Controlled
376   Diameters. *IEEE Trans. Ind. Appl.* **2019**, *55* (5), 5239–5243.
377   https://doi.org/10.1109/TIA.2019.2920811.

378   (18)   Rubin Pedrazzo, A.; Cecone, C.; Morandi, S.; Manzoli, M.; Bracco, P.; Zanetti, M.
379   Nanosized Sno2 Prepared by Electrospinning: Influence of the Polymer on Both
380   Morphology and Microstructure. *Polymers (Basel).* **2021**, *13* (6).
381   https://doi.org/10.3390/polym13060977.

382   (19)   Fioravanti, A.; Morandi, S.; Rubin Pedrazzo, A.; Bracco, P.; Zanetti, M.; Manzoli, M.;
383   Mazzocchi, M.; Carotta, M. C. Ultrasensitive Gas Sensors Based on Electrospun TiO2 and
384   ZnO. *Proceedings* **2017**, *1* (4), 485. https://doi.org/10.3390/proceedings1040485.

385   (20)   Wang, X.; Fan, H.; Ren, P. Electrospinning Derived Hollow SnO2 Microtubes with Highly
386   Photocatalytic Property. *Catal. Commun.* **2013**, *31*, 37–41.
387   https://doi.org/10.1016/j.catcom.2012.11.009.

388   (21)   Sun, X.; Huang, Y.; Zong, M.; Wu, H.; Ding, X. Preparation of Porous SnO2/ZnO
389   Nanotubes via a Single Spinneret Electrospinning Technique as Anodes for Lithium Ion
390   Batteries. *J. Mater. Sci. Mater. Electron.* **2016**, *27* (3), 2682–2686.
391   https://doi.org/10.1007/s10854-015-4077-x.

392   (22)   Sun, Y.; Wang, J.; Du, H.; Li, X.; Wang, C.; Hou, T. Formaldehyde Gas Sensors Based on
393   SnO2/ZSM-5 Zeolite Composite Nanofibers. *J. Alloys Compd.* **2021**, *868*, 159140.
394   https://doi.org/10.1016/j.jallcom.2021.159140.

395   (23)   Kurkov, S. V.; Loftsson, T. Cyclodextrins. *Int. J. Pharm.* **2013**, *453* (1), 167–180.

396   https://doi.org/10.1016/j.ijpharm.2012.06.055.

(24) Duchêne, D. Cyclodextrins and Their Inclusion Complexes. *Cyclodextrins Pharm. Cosmet. Biomed. Curr. Futur. Ind. Appl.* **2011**, 1–18. https://doi.org/10.1002/9780470926819.ch1.

(25) Szejtli, J. Introduction and General Overview of Cyclodextrin Chemistry. *Chem. Rev.* **1998**, *98* (5), 1743–1754. https://doi.org/10.1021/cr970022c.

(26) Szejtli, J. Utilization of Cyclodextrins in Industrial Products and Processes. *J. Mater. Chem.* **1997**, *7* (4), 575–587. https://doi.org/10.1039/a605235e.

(27) Loftsson, T.; Duchêne, D. Cyclodextrins and Their Pharmaceutical Applications. *Int. J. Pharm.* **2007**, *329* (1–2), 1–11. https://doi.org/10.1016/j.ijpharm.2006.10.044.

(28) Szejtli, J. *Cyclodextrin Technology*; s.l.:Springer Netherlands, 1988.

(29) Marques, H. M. C. A Review on Cyclodextrin Encapsulation of Essential Oils and Volatiles. *Flavour Fragr. J.* **2010**, *25* (5), 313–326. https://doi.org/10.1002/ffj.2019.

(30) Saenger, W. Cyclodextrin Inclusion Compounds in Research and Industry. *Angew. Chemie Int. Ed. English* **1980**, *19* (5), 344–362. https://doi.org/10.1002/anie.198003441.

(31) Prochowicz, D.; Kornowicz, A.; Lewiński, J. Interactions of Native Cyclodextrins with Metal Ions and Inorganic Nanoparticles: Fertile Landscape for Chemistry and Materials Science. *Chem. Rev.* **2017**, *117* (22), 13461–13501. https://doi.org/10.1021/acs.chemrev.7b00231.

(32) Norkus, E. Metal Ion Complexes with Native Cyclodextrins. An Overview. *J. Incl. Phenom. Macrocycl. Chem.* **2009**, *65* (3), 237–248. https://doi.org/10.1007/s10847-009-9586-x.

(33) Erem Bilensoy. *Cyclodextrins in Pharmaceutics, Cosmetics, and Biomedicine: Current and Future Industrial Applications*; John Wiley and Sons Inc, Ed.; 2011.

(34) Zhang, J.; Xu, D.; Qian, W.; Zhu, J.; Yan, F. Host-Guest Inclusion Complexes Derived Heteroatom-Doped Porous Carbon Materials. *Carbon N. Y.* **2016**, *105*, 183–190. https://doi.org/10.1016/j.carbon.2016.04.034.

421   (35)   Q. Qi, T. Zhang, L. L. and X. Z. Synthesis and Toluene Sensing Properties of SnO2
422   Nanofibers. *Sensors Actuators B Chem.* **2009**, *137*, 471.

423   (36)   Wang, W.; Huang, H.; Li, Z.; Zhang, H.; Wang, Y.; Zheng, W.; Wang, C. Zinc Oxide
424   Nanofiber Gas Sensors via Electrospinning. *J. Am. Ceram. Soc.* **2008**, *91* (11), 3817–3819.
425   https://doi.org/10.1111/j.1551-2916.2008.02765.x.

426   (37)   Anastas, P. T.; Warner, J. C. *Green Chemistry: Theory and Practice*; Oxford University
427   Press, 1998.

428   (38)   Anastas, P. T.; Zimmerman, J. B. Design through the 12 Principles of Green Engineering.
429   *IEEE Eng. Manag. Rev.* **2007**, *35* (3), 16. https://doi.org/10.1109/EMR.2007.4296421.

430   (39)   Verma, S.; Rawat, A.; Kaul, M.; Saini, S. Solid Dispersion: A Strategy for Solubility
431   Enhancement. *Int. J. Pharm. Technol.* **2011**, *3* (2), 1062–1099.

432   (40)   Patil, J. S.; Kadam, D. V.; Marapur, S. C.; Kamalapur, M. V. Inclusion Complex System; a
433   Novel Technique to Improve the Solubility and Bioavailability of Poorly Soluble Drugs: A
434   Review. *Int. J. Pharm. Sci. Rev. Res.* **2010**, *2* (2), 29–34.

435   (41)   Crini, G. Recent Developments in Polysaccharide-Based Materials Used as Adsorbents in
436   Wastewater   Treatment.   *Prog.   Polym.   Sci.*   **2005**,   *30*   (1),   38–70.
437   https://doi.org/10.1016/j.progpolymsci.2004.11.002.

438   (42)   Loftsson, T.; Saokham, P.; Sá Couto, A. R. Self-Association of Cyclodextrins and
439   Cyclodextrin Complexes in Aqueous Solutions. *Int. J. Pharm.* **2019**, *560* (5), 228–234.
440   https://doi.org/10.1016/j.ijpharm.2019.02.004.

441   (43)   Loftsson, T.; Magnúsdóttir, A.; Másson, M.; Sigurjónsdóttir, J. F. Self-Association and
442   Cyclodextrin Solubilization of Drugs. *J. Pharm. Sci.* **2002**, *91* (11), 2307–2316.
443   https://doi.org/10.1002/jps.10226.

444   (44)   Mazzaglia, A.; Sciortino, M. T.; Kandoth, N.; Sortino, S. Cyclodextrin-Based
445   Nanoconstructs for Photoactivated Therapies. *J. Drug Deliv. Sci. Technol.* **2012**, *22* (3),
446   235–242. https://doi.org/10.1016/S1773-2247(12)50034-1.

447   (45)   Zhang, J.; Ma, P. X. Cyclodextrin-Based Supramolecular Systems for Drug Delivery:
448   Recent Progress and Future Perspective. *Adv. Drug Deliv. Rev.* **2013**, *65* (9), 1215–1233.
449   https://doi.org/10.1016/j.addr.2013.05.001.

450   (46)   Brochsztain, S.; Politi, M. J. Solubilization of 1,4,5,8- Naphthalenediimides and 1, 8-
451   Naphthalimides through the Formation of Novel Host–Guest Complexes with a-
452   Cyclodextrin. *Langmuir* **1999**, *15*, 486–4494.

453   (47)   Mar, G. L.; Timbrell, P. Y.; Lamb, R. N. Formation of Zinc Oxide Thin Films by the
454   Thermal Decomposition of Zinc Acetate. **1993**, *73*, 177–192. https://doi.org/10.1007/978-
455   3-642-84933-6_15.

456   (48)   Trotta, F.; Zanetti, M.; Camino, G. Thermal Degradation of Cyclodextrins. **2000**, *69*, 373–
457   379.

458

459   TOC/GRAPHIC ABSTRACT

464

465   SYNOPSIS